

APMA 935: Assignment 2

Mantej Sokhi

February 12, 2026

1a)

Proof. We know for the advection equation $u_t + au_x = 0$. Over a time interval of length $2\Delta t$ so from t^{n-1} to t^{n+1} , the solution at (x_j, t^{n+1}) depends on data from the initial point $\hat{x} = x_j - a(t^{n+1} - t^{n-1}) = x_j - 2a\Delta t$. So, the spatial dependence spans a maximum distance of $|\hat{x} - x_j| = 2|a|\Delta t$.

The numerical scheme in question is 2 step in time and at time step n , the spatial derivative u_x depends on grid points $U_{j-2}, U_{j-1}, U_{j+1}$ and U_{j+2} which is at max 2 grid points of j . Note, the time step itself also depends on time $n-1$ values within 2 grid points of j so to compute U_j^{n+1} depends on Δt ranging from $n-1$ to $n+1$ and grid points $U_{j-4}, U_{j-2}, U_j, U_{j+2}$ and U_{j+4} . Hence, the numerical domain of dependence over $t^{n-1} \rightarrow t^{n+1}$ reaches a maximum distance of $4\Delta x$ from its initial point x_j . We know that PDE dependence should be contained within the numerical dependence which implies $2|a|\Delta t \leq 4\Delta x$. Now, dividing both sides by 2 we get $|a|\Delta t \leq 2\Delta x \implies \frac{|a|\Delta t}{\Delta x} \leq 2 \implies |\sigma| \leq 2$.

Hence, we have shown that CFL condition for this scheme is $|\sigma| \leq 2$, where $\sigma = \frac{a\Delta t}{\Delta x}$ as usual. \square

1b) We are looking for a Fourier mode solution of the form $U_j^n = \xi^n e^{ij\theta}$ where $\theta \in [-\pi, \pi]$ and $\xi = \xi(\theta)$ is the amplification factor. Substituting this into our CTCS type scheme where we are letting $U_{j\pm 1}^n = U_j^n e^{\pm i\theta}$ and $U_{j\pm 2}^n = U_j^n e^{\pm 2i\theta}$ gives us $\frac{\xi - \xi^{-1}}{2\Delta t} + \frac{ia}{\Delta x} \left(\frac{4}{3} \sin \theta - \frac{1}{6} \sin(2\theta) \right) = 0$. Note, $\sin(2\theta) = 2 \sin \theta \cos \theta$ and let $\sigma = \frac{a\Delta t}{\Delta x}$. Plugging this back into our equation we get $\xi - \xi^{-1} + 2i\sigma \Phi(\theta) = 0$ where $\Phi(\theta) = \frac{1}{3} \sin \theta (4 - \cos \theta)$. Now, we can multiply our equation by ξ which gives us $\xi^2 + 2i\sigma\Phi(\theta)\xi - 1 = 0 \implies \xi = -i\sigma\Phi(\theta) \pm \sqrt{1 - \sigma^2\Phi(\theta)^2}$. Note, this is a quadratic equation and since the constant term is -1 , the two roots satisfy $|\xi_1||\xi_2| = 1 \implies$ stable. However, this only occurs when $1 - \sigma^2\Phi(\theta)^2 \geq 0 \forall \theta$ and $|\sigma\Phi(\theta)| \leq 1 \forall \theta$ which means this is only satisfied when both roots lie on the unit circle which occurs precisely when the square root is real. Hence the stability restriction on σ is precisely $|\sigma| \leq \frac{1}{\max_{\theta \in [-\pi, \pi]} |\Phi(\theta)|}$.

We will now compute the maximum and show this is ≈ 0.7288 . Note that $\Phi(\theta)$ is odd and nonnegative on $[0, \pi]$, so it is sufficient to maximize $\Phi(\theta)$ on $[0, \pi]$. Differentiating gives us $\Phi'(\theta) = \frac{1}{3}(4 \cos \theta + 1 - 2 \cos^2 \theta)$. Now, let $\Phi'(\theta) = 0$ and $c = \cos \theta$. Substituting this into the above equation gives us $4c + 1 - 2c^2 = 0 \implies 2c^2 - 4c - 1 = 0 \implies \bar{c} = 1 - \frac{\sqrt{6}}{2} \in [-1, 1]$. Therefore, $\Phi_{\max} = \Phi(\bar{\Theta}) = \frac{1}{3}\sqrt{1 - \bar{c}^2}(4 - \bar{c}) \approx 1.37222$ and $\sigma_* = \frac{1}{\Phi_{\max}} \approx 0.7288 \implies |\sigma| \leq \sigma_* \approx 0.7288$.

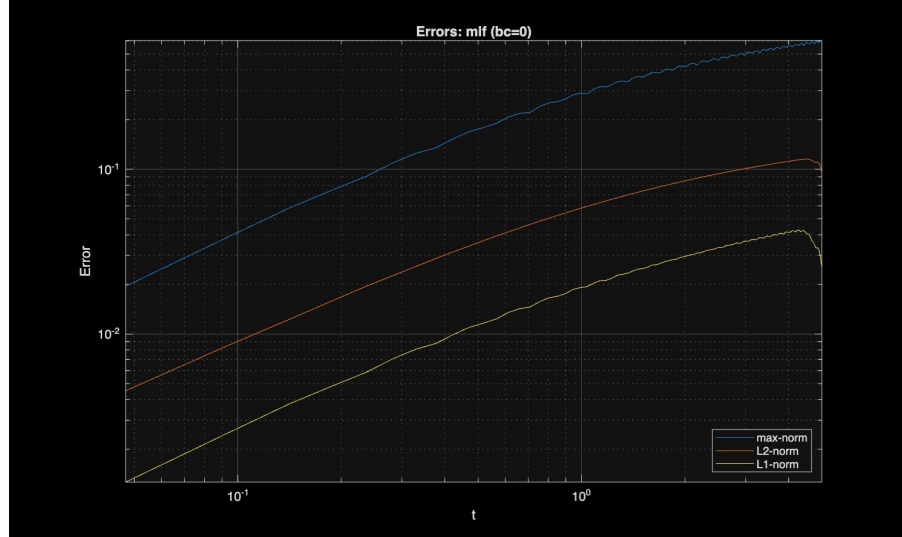
Hence, we have performed von Neumann stability analysis of the method and shown that the stability restriction is $|\sigma| \leq \sigma_* \approx 0.7288$.

1c) Let $u(x, t)$ be a smooth exact solution of $u_t + au_x = 0$. To obtain the local truncation error τ_j^n we will substitute the values $u_j^n = u(x_j, t^n)$ into the finite difference scheme. This gives us $\tau_j^n = \frac{u_j^{n+1} - u_j^{n-1}}{2\Delta t} + a \left[\frac{4}{3} \frac{u_{j+1}^n - u_{j-1}^n}{2\Delta x} - \frac{1}{3} \frac{u_{j+2}^n - u_{j-2}^n}{4\Delta x} \right]$. Now, Taylor expanding with (x_j, t^n) gives us $\frac{u_j^{n+1} - u_j^{n-1}}{2\Delta t} = u_t(x_j, t^n) + \frac{\Delta t^2}{6} u_{ttt}(x_j, t^n) + \mathcal{O}(\Delta t^4)$.

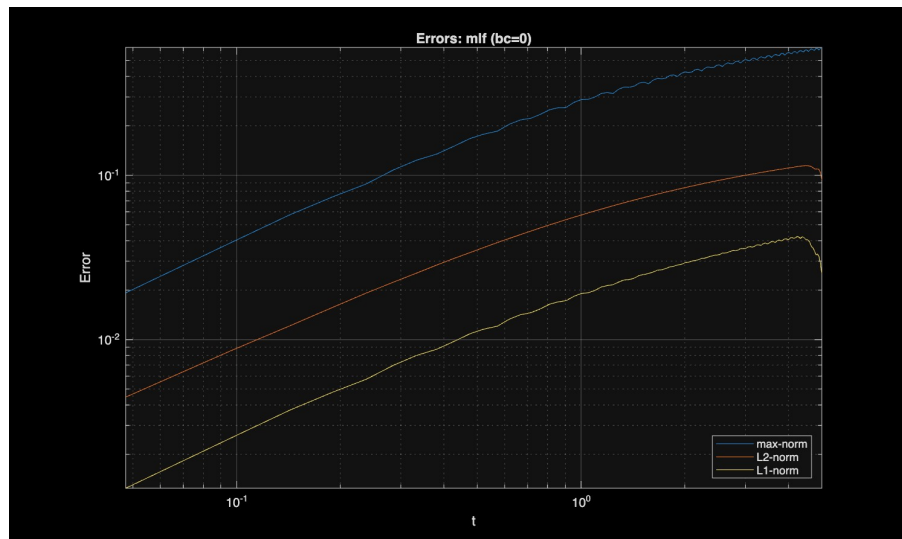
Now let the spatial operator be written as a linear combination of centered differences which is $\frac{4}{3} \frac{u_{j+1} - u_{j-1}}{2\Delta x} - \frac{1}{3} \frac{u_{j+2} - u_{j-2}}{4\Delta x}$. We will now expand each of them individually. So, $\frac{u_{j+1} - u_{j-1}}{2\Delta x} = u_x + \frac{\Delta x^2}{6} u_{xxx} + \frac{\Delta x^4}{120} u_{xxxxx} + \mathcal{O}(\Delta x^6)$ and $\frac{u_{j+2} - u_{j-2}}{4\Delta x} = u_x + \frac{4\Delta x^2}{6} u_{xxx} + \frac{16\Delta x^4}{120} u_{xxxxx} + \mathcal{O}(\Delta x^6)$. However, we can cancel the Δx^2 term and we get $\frac{4}{3} \frac{u_{j+1} - u_{j-1}}{2\Delta x} - \frac{1}{3} \frac{u_{j+2} - u_{j-2}}{4\Delta x} = u_x - \frac{\Delta x^4}{30} u_{xxxxx} + \mathcal{O}(\Delta x^6)$. We can now substitute these values into τ_j^n and using the linear advection equation in the question we can cancel the leading terms which gives us $\tau_j^n = \frac{\Delta t^2}{6} u_{ttt} - a \frac{\Delta x^4}{30} u_{xxxxx} + \mathcal{O}(\Delta t^4) + \mathcal{O}(\Delta x^6)$. We now differentiate the PDE as shown in class to express u_{ttt} in terms of spatial derivatives and we get $u_t = -au_x \Rightarrow u_{tt} = a^2 u_{xx} \Rightarrow u_{ttt} = -a^3 u_{xxx}$. Therefore, $\tau_j^n = -\frac{a^3 \Delta t^2}{6} u_{xxx} - \frac{a \Delta x^4}{30} u_{xxxxx} + \mathcal{O}(\Delta t^4) + \mathcal{O}(\Delta x^6)$.

Note, the leading error terms involve odd spatial derivatives u_{xxx} and u_{xxxxx} . Odd derivatives are primarily known to change the phase speed of phase errors so we should not expect any smoothness near a steep gradient but rather the error to be dispersive.

1d) We performed a von Neumann stability analysis of the given method in part(b) and showed that the stability restriction is $|\sigma| \leq \sigma_* \approx 0.7288$. This behavior was clearly observed in the numerical tests performed. For values of σ below ≈ 0.73 the solution was bounded and the error growth was mild. However, for σ values above this threshold (> 0.75) the error norms increased significantly over time and the numerical solution deviated strongly from the exact solution. Therefore, we can conclude that our tests confirm that the practical stability threshold is close to σ_* rather than the CFL bound from part (a).

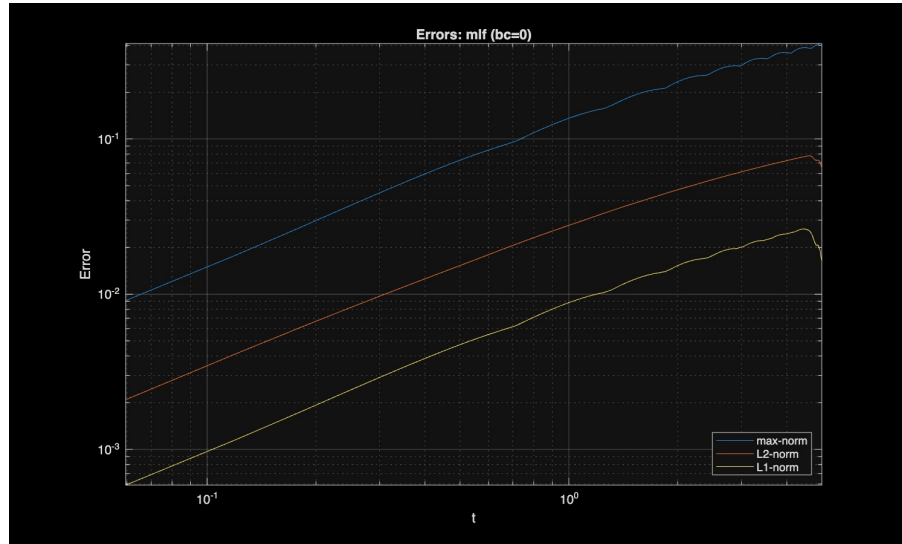


(a) Errors for $\sigma = 0.71$

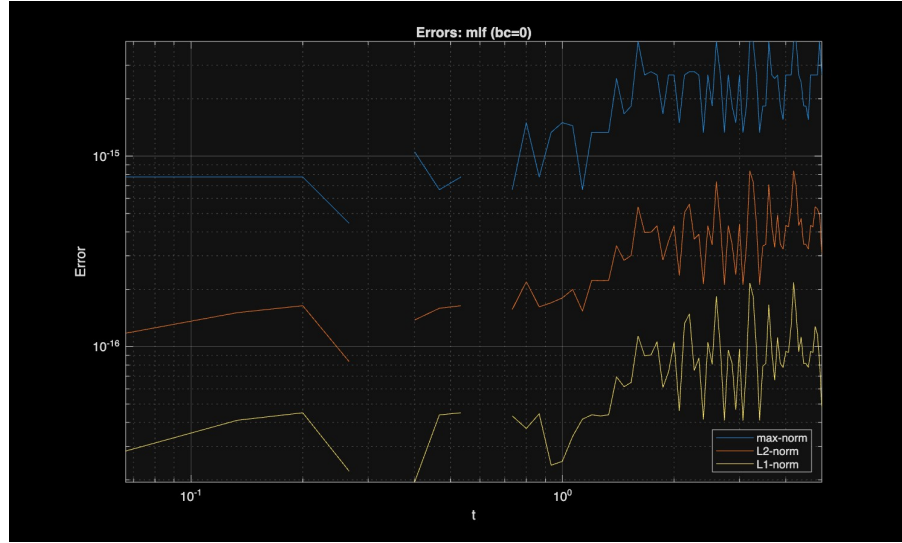


(b) Errors for $\sigma = 0.72$

Figure 1: L_1 , L_2 and L_∞ errors for $\sigma = 0.71$ and 0.72 for the modified Leap-Frog scheme



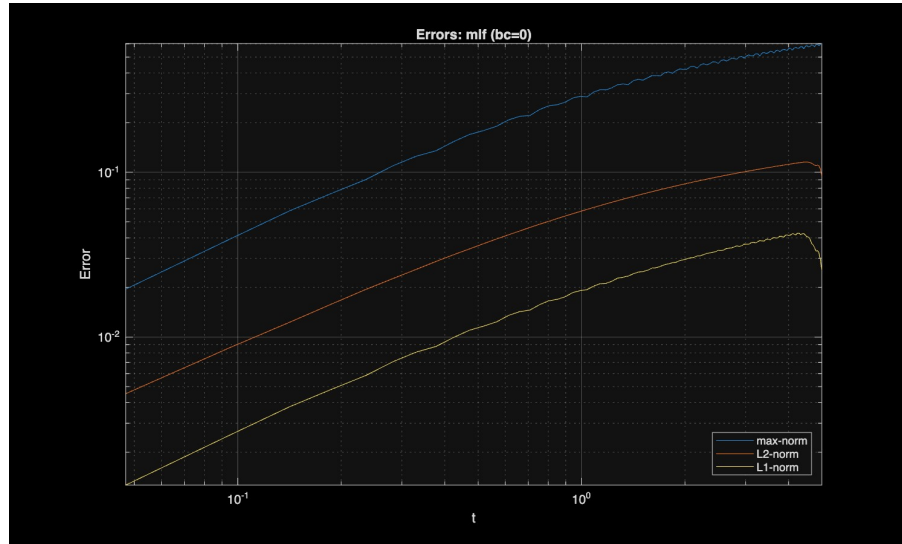
(a) Errors for $\sigma = 0.9$



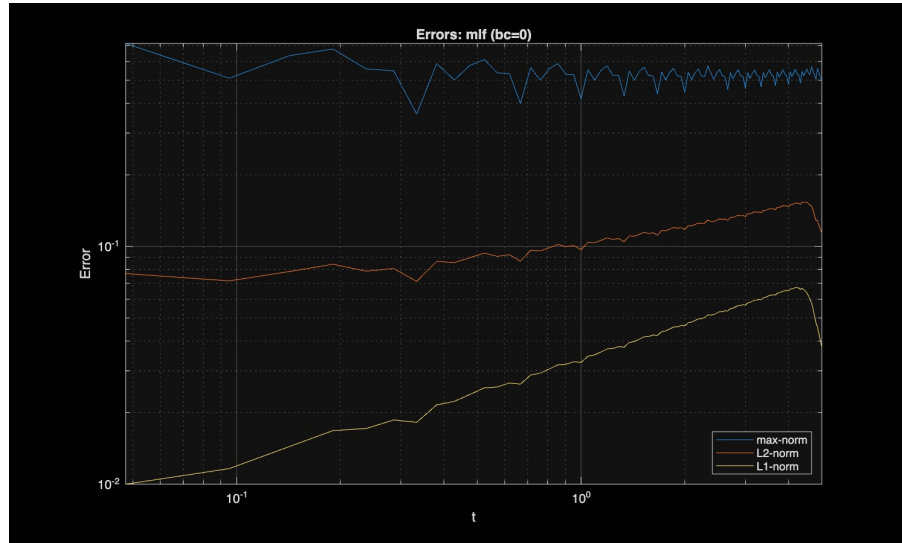
(b) Errors for $\sigma = 1.0$

Figure 2: L_1 , L_2 and L_∞ errors for $\sigma = 0.9$ and 1.0 for the modified Leap-Frog scheme

From, observation we can see that for smooth initial data, the wave shape stays preserved but exhibits phase error and dispersion. For non smooth ic's, we observe oscillations near the discontinuity as σ gets closer to ≈ 0.7288 . Our modified leap frog scheme makes use of a higher order spatial derivative i.e., it exhibits less diffusion as long as $\sigma < 0.7288$ when compared with the leap frog scheme. On the other hand, FTBS is stable for $0 \leq \sigma \leq 1$ but is more diffusive. Lastly, Fromme more or less tends to reduce oscillations for non smooth ic's and is essentially a good compromise if choosing between dispersion and diffusion.



(a) Errors for $\sigma = 0.71$ with IC=0



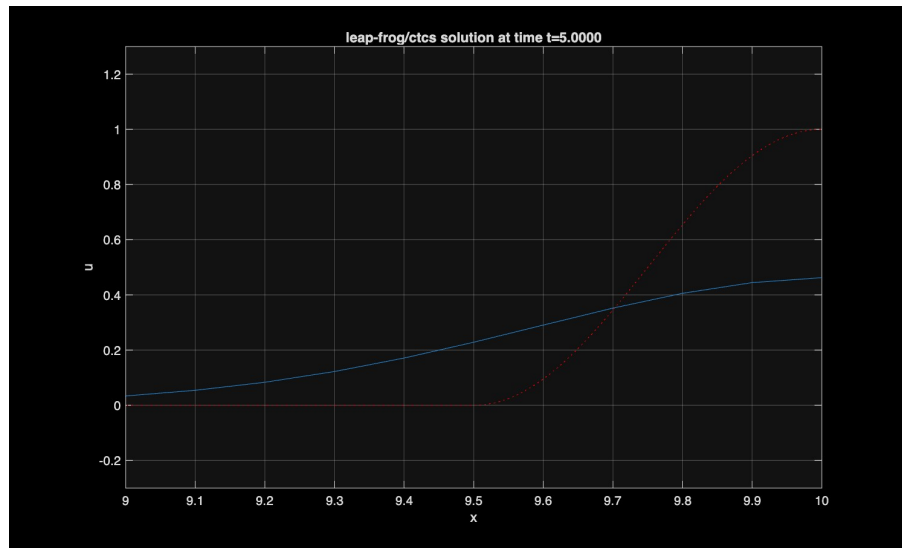
(b) Errors for $\sigma = 0.71$ with IC=1

Figure 3: L_1, L_2 and L_∞ errors for $\sigma = 0.71$ with IC's=1 and 2 for the modified Leap-Frog scheme

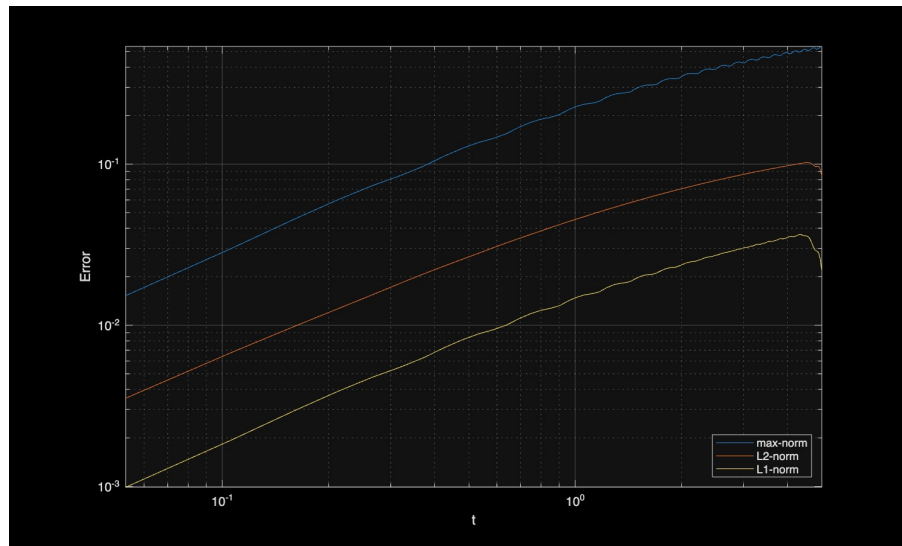
Code for modified Leap-Frog scheme.

2a) For the linear advection equation $u_t + au_x = 0$ where $a > 0$ the wave travels to the right $x - at = c$ for some constant c which implies that the right boundary $x = x_{\max}$ is an outflow boundary. CTCS is largely non-dissipative but dispersive so boundary induced disturbances tend to produce oscillatory ripples. Fromm is typically less diffusive but it still responds strongly near $U_M = 0$ due to the nature of its wider stencil.

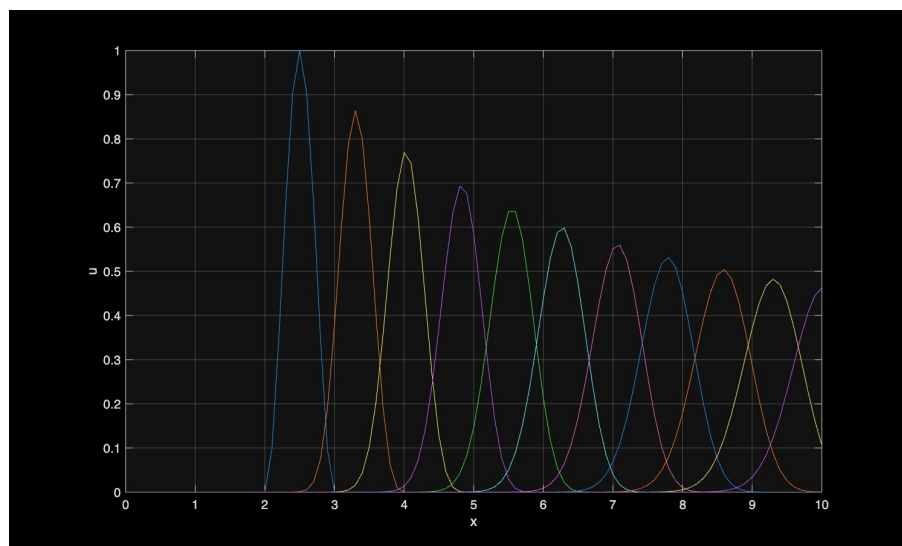
In the provided code, the CTCS and Fromm schemes involves a U_{j+1}^n term and this cannot be applied directly at the last grid point $j = M$ without having a value for outside the domain. Instead, the code sets $u_M = 0$, which becomes inconsistent once the wave reaches x_{\max} . This fictitious value introduces a steep gradient near the boundary which in turn generates oscillations and a sharp spike in the error the instant the wave first touches the boundary.



(a) Solution plot of the CTCS scheme

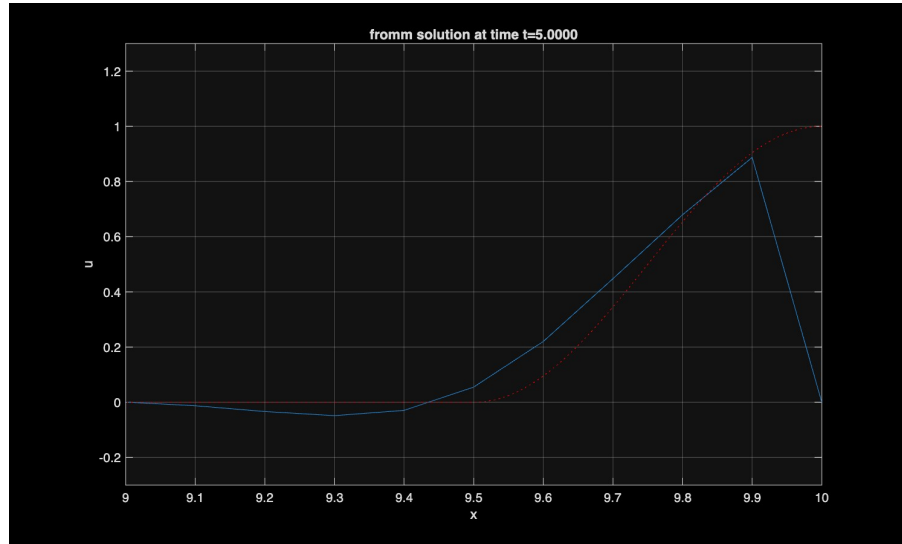


(b) L_1 , L_2 and L_∞ plots of the CTCS scheme

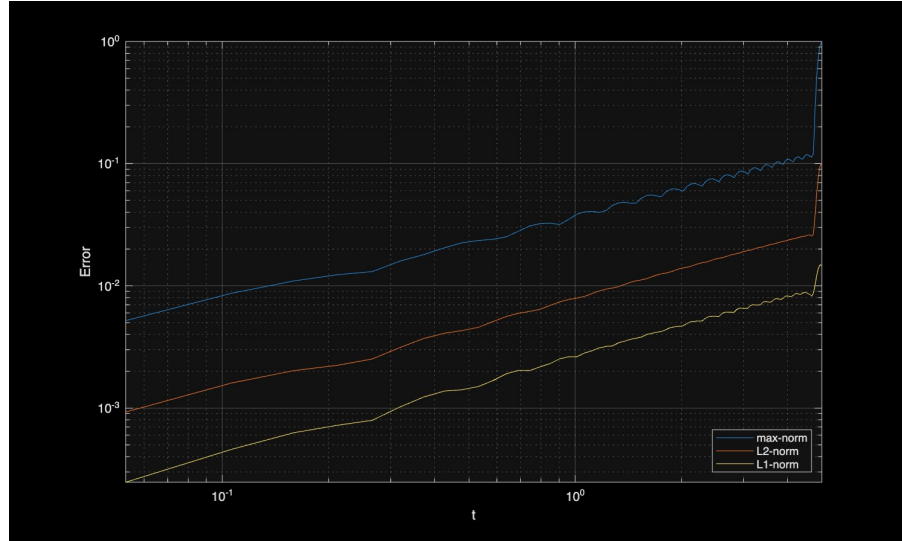


(c) Solution plots at varying t for CTCS scheme

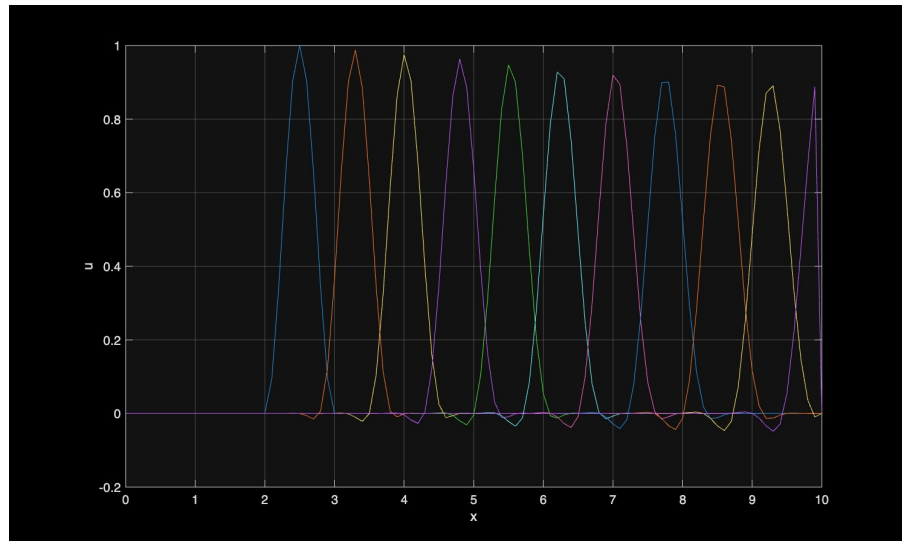
Figure 4: CTCS scheme plots



(a) Solution plot of the Fromme scheme



(b) L_1, L_2 and L_∞ plots of the Fromme scheme



(c) Solution plots for varying t for Fromme scheme

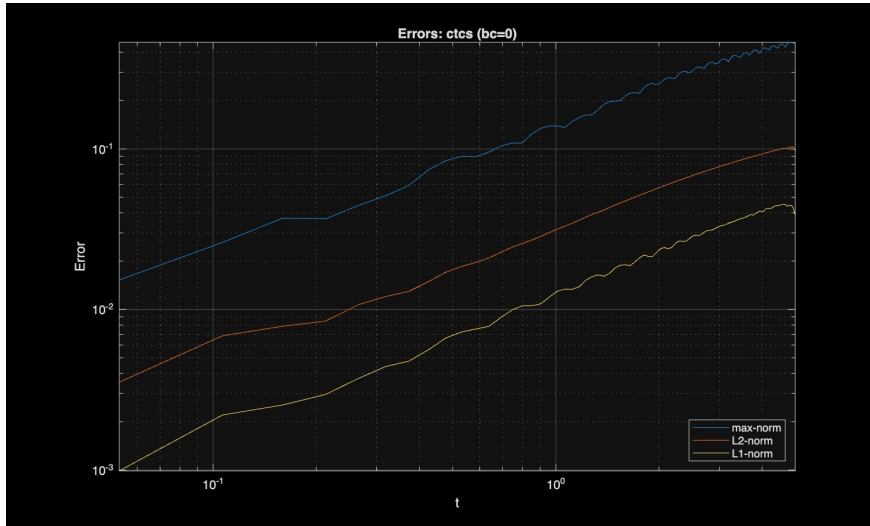
Figure 5: Fromme scheme plots

2b) Let the grid be uniform with spacing Δx and let the shifted coordinate be defined as $\xi = \frac{x-x_M}{\Delta x}$. Then points U_M, U_{M_1}, U_{M_2} and U_{M+1} correspond to $\xi = 0$ (x_M), $\xi = -1$ (x_{M-1}), $\xi = -2$ (x_{M-2}) and $\xi = 1$ (x_{M+1}).

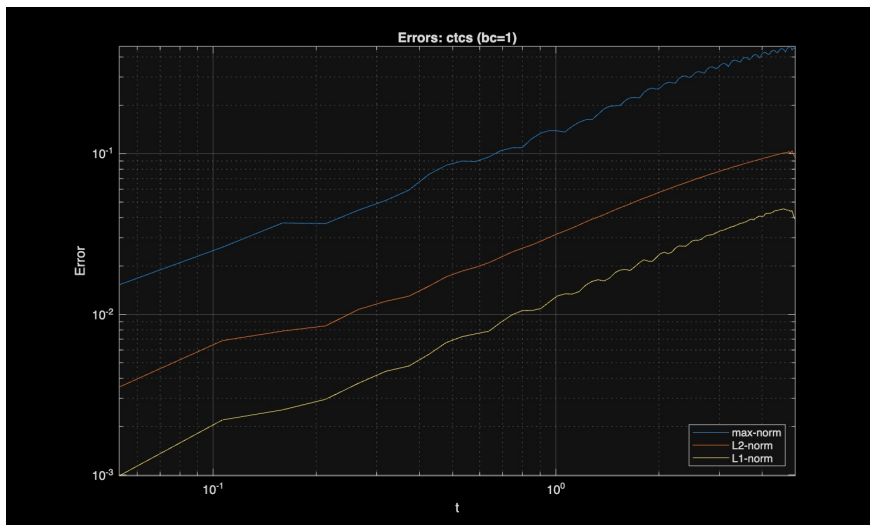
For a linear extrapolation we want to fit a line through the two right most interior points $(\xi, U) = (0, U_M)$ and $(-1, U_{M-1})$. The slope is $\frac{U_M - U_{M-1}}{0 - (-1)} = U_M - U_{M-1}$, so the linear interpolant then is $U(\xi) = U_M + (U_M - U_{M-1})\xi$. Now, evaluating this at $\xi = 1$ we get $U_{M+1} = U(1) = U_M + (U_M - U_{M-1}) = 2U_M - U_{M-1}$. Hence, in the form $U_{M+1} = aU_M + bU_{M-1}$ the coefficients are $a = 2, b = -1$ and $c = 0$.

For a quadratic extrapolation we want to fit a line through three interior points $\xi = 0, -1, -2$ and we will use Lagrange interpolation. Let $U(\xi) = U_M L_0(\xi) + U_{M-1} L_1(\xi) + U_{M-2} L_2(\xi)$ where $L_0(\xi) = \frac{(\xi+1)(\xi+2)}{(0+1)(0+2)} = \frac{(\xi+1)(\xi+2)}{2}$, $L_1(\xi) = \frac{\xi(\xi+2)}{(-1-0)(-1+2)} = -\xi(\xi+2)$, and $L_2(\xi) = \frac{\xi(\xi+1)}{(-2-0)(-2+1)} = \frac{\xi(\xi+1)}{2}$. Evaluating the above three at $\xi = 1$ gives us $L_0(1) = 3, L_1(1) = -3$ and $L_2(1) = 1$, and therefore $U_{M+1} = U(1) = 3U_M - 3U_{M-1} + U_{M-2}$. Hence, in the form $U_{M+1} = aU_M + bU_{M-1} + cU_{M-2}$ the coefficients are $a = 3, b = -3$ and $c = 1$.

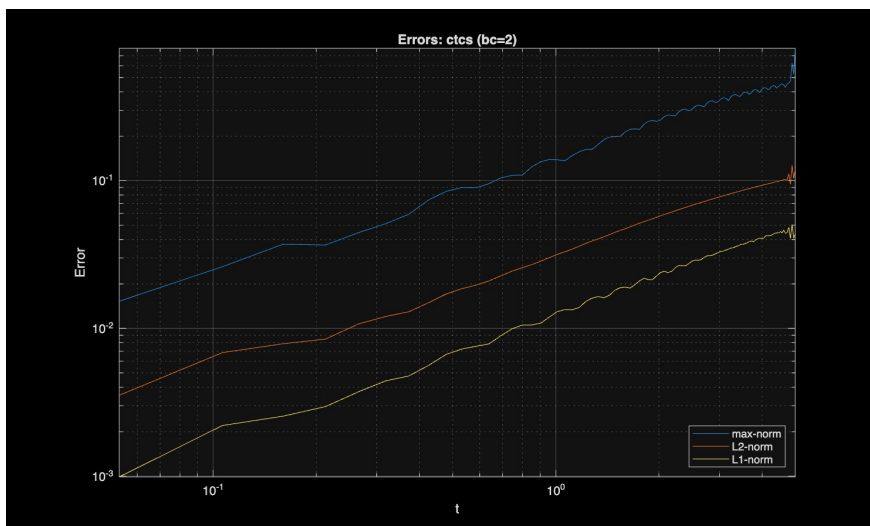
2c)



(a) Error plot w/ BC=0

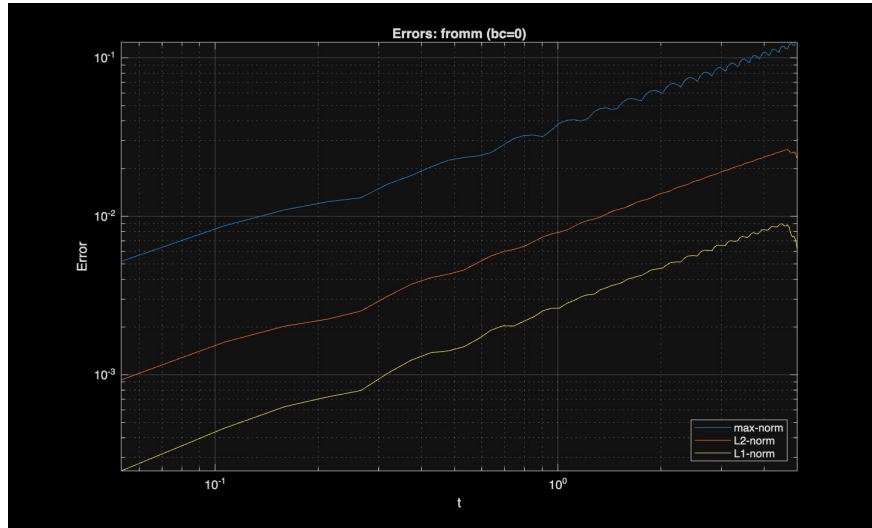


(b) Error plot w/ BC=1

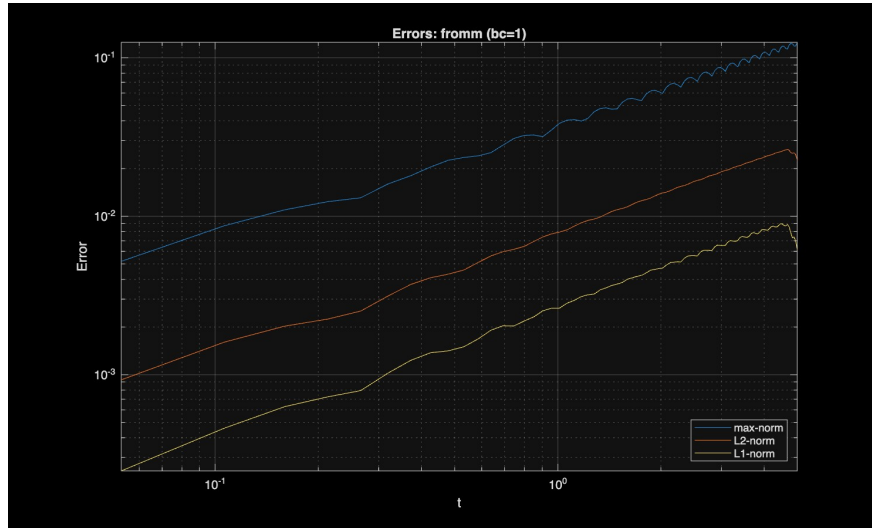


(c) Error plot w/ BC=2

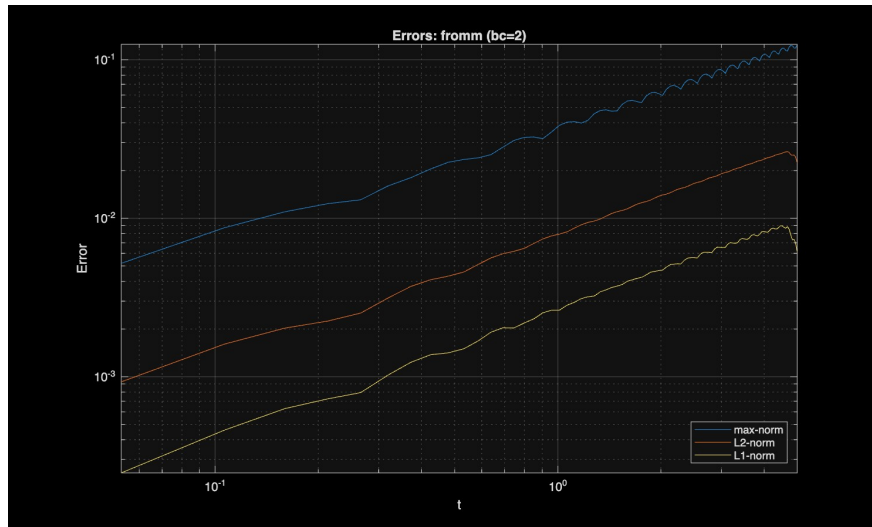
Figure 6: CTCS scheme error plots for L_1 , L_2 and L_∞



(a) Error plot w/ BC=0

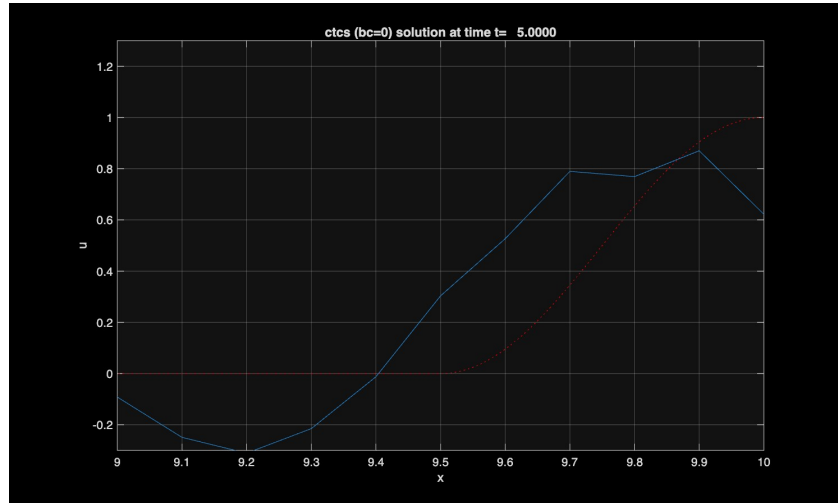


(b) Error plot w/ BC=1

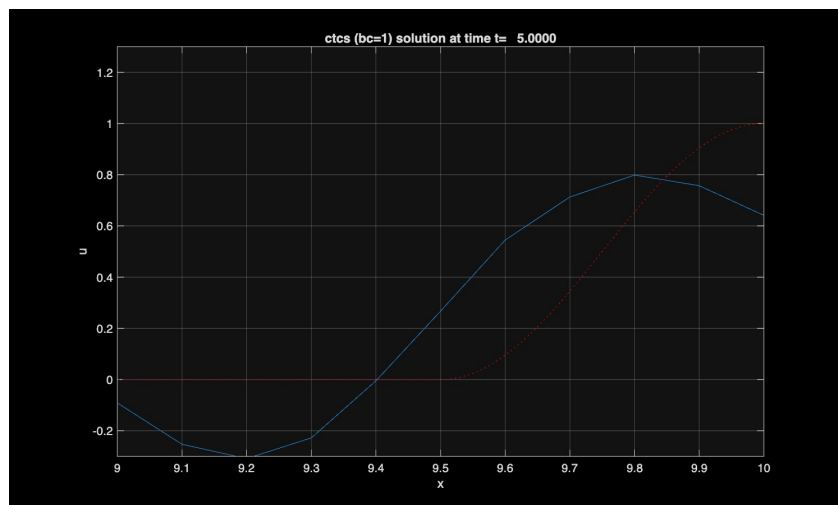


(c) Error plot w/ BC=2

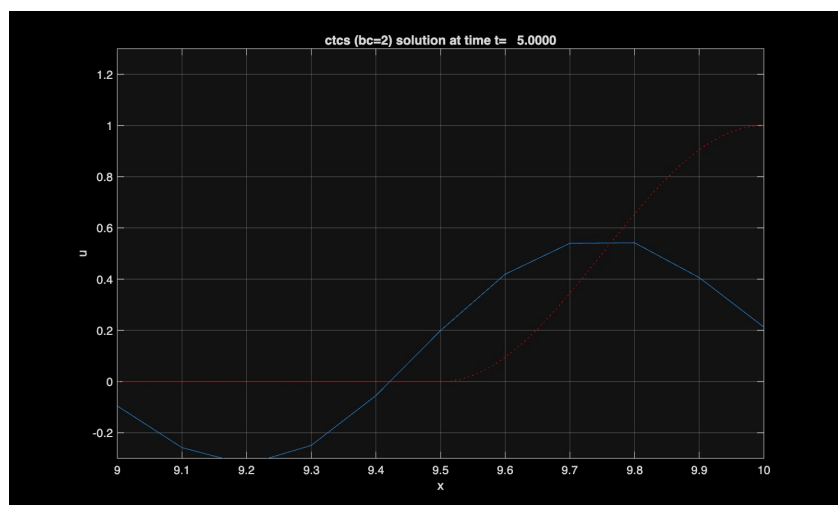
Figure 7: Fromme scheme error plots for L_1 , L_2 and L_∞



(a) Solution plot w/ BC=0

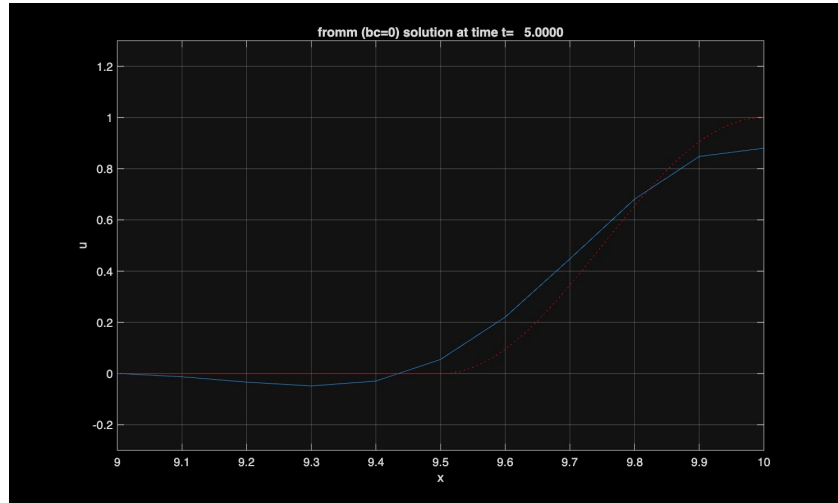


(b) Solution plot w/ BC=1

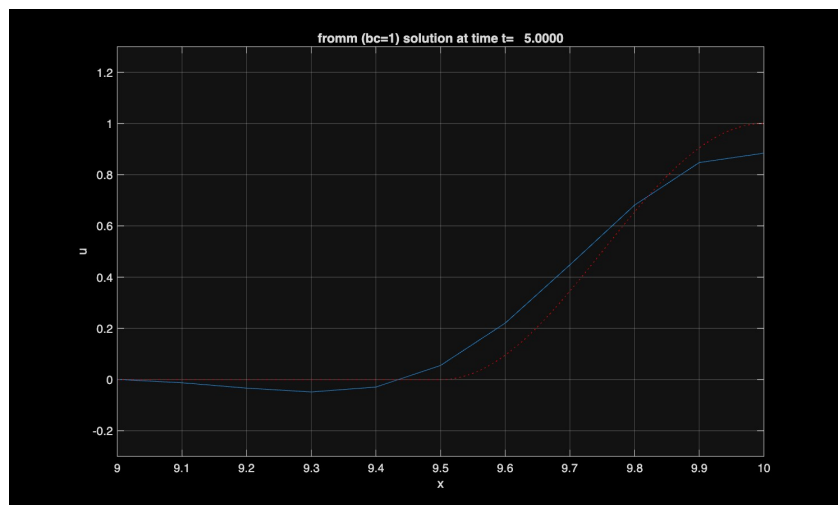


(c) Solution plot w/ BC=2

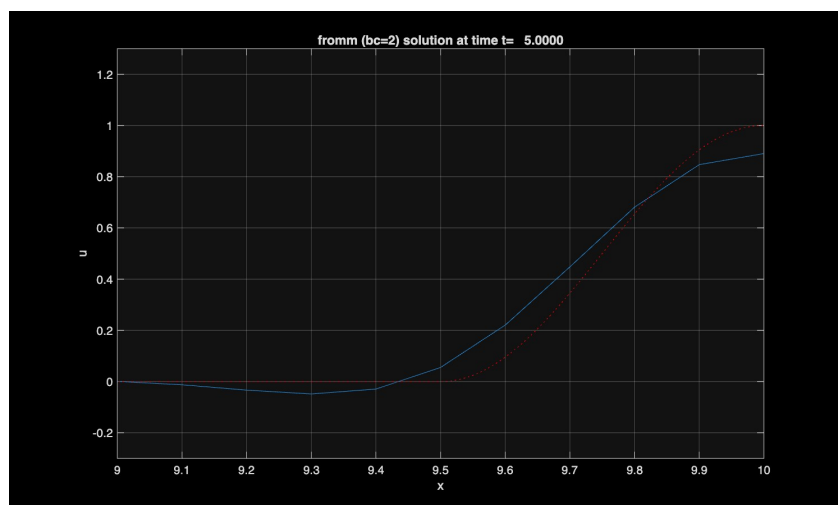
Figure 8: CTCS solution plots



(a) Solution plot w/ BC=0

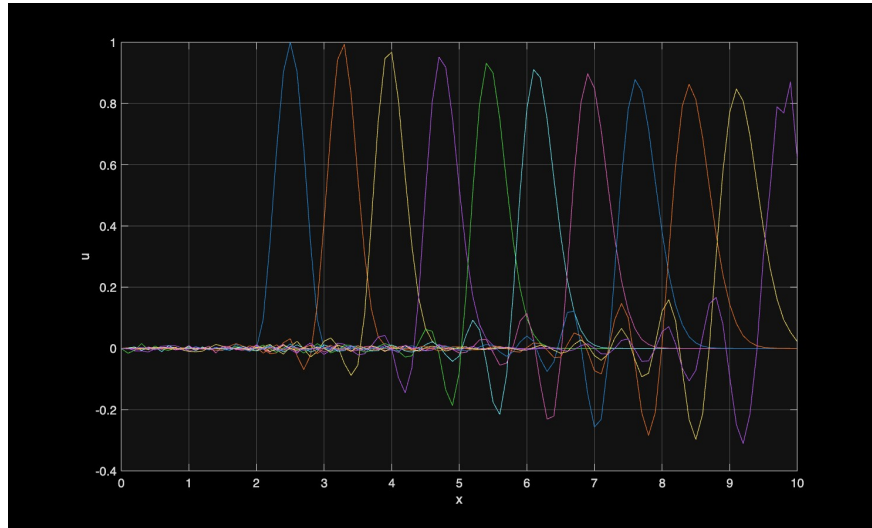


(b) Solution plot w/ BC=1

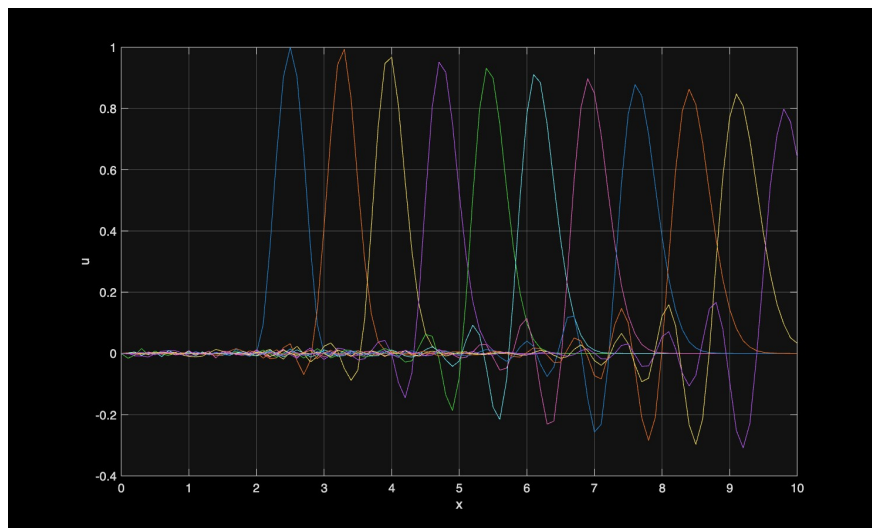


(c) Solution plot w/ BC=2

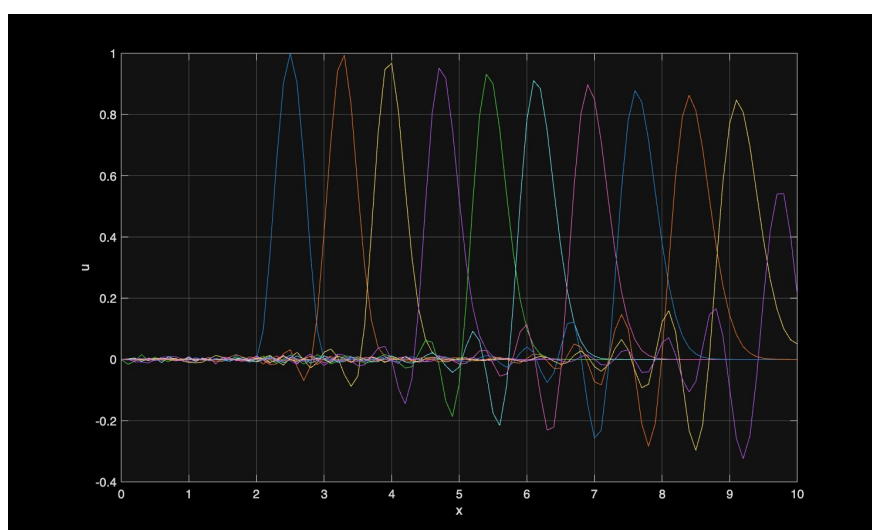
Figure 9: Fromm solution plots



(a) Solution plots for varying t for BC=0

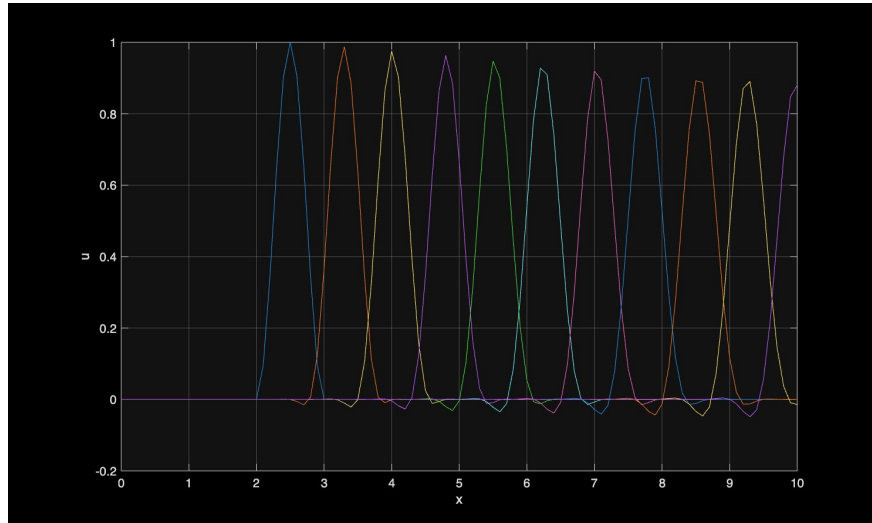


(b) Solution plots for varying t for BC=1

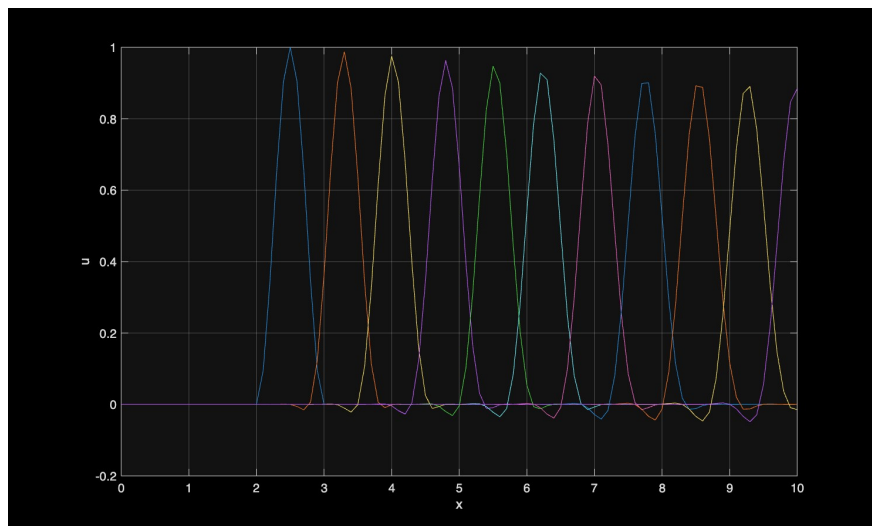


(c) Solution plots for varying t for BC=2

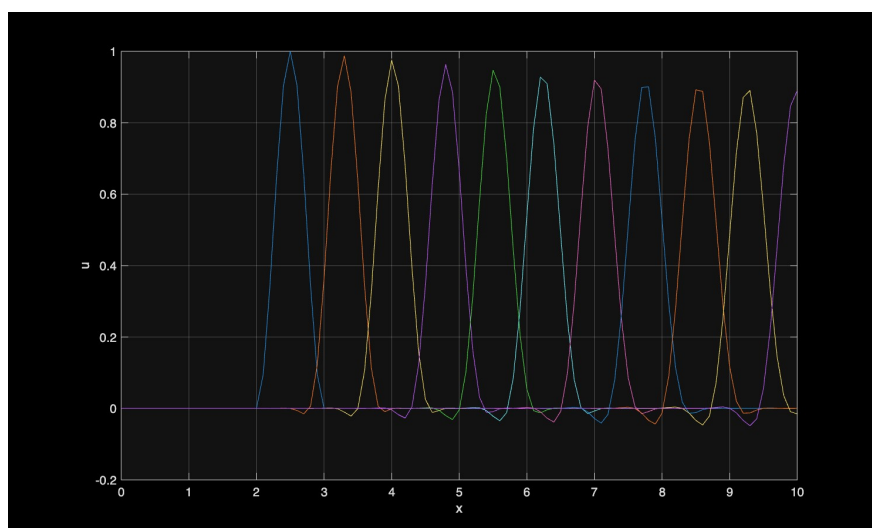
Figure 10: Solution profiles from the CTCS scheme for BC=0,1 and 2 respectively.



(a) Solution plots for varying t for BC=0



(b) Solution plots for varying t for BC=1



(c) Solution plots for varying t for BC=2

Figure 11: Solution profiles from the Fromme scheme for BC=0,1 and 2 respectively.

Code for extrapolation conditions.

3a) We need a forward difference in time for $\frac{\partial u}{\partial t}$. Using Taylor series expansion at $t = t_i$ we have $u(x, t + \Delta t) = u(x, t) + \frac{\Delta t \partial u}{\partial t} + \frac{(\Delta t)^2 \partial^2 u}{2! \partial t^2} + \mathcal{O}((\Delta t)^3)$. We drop the error terms and isolate $\frac{\partial u}{\partial t}$ and obtain $\frac{\partial u}{\partial t} = \frac{u(x, t + \Delta t) - u(x, t)}{\Delta t} \approx \frac{u_i^{n+1} - u_i^n}{\Delta t}$.

We need a first order upwind difference for $\frac{\partial u}{\partial x}$. Again, using taylor series expansion at $x = x_i$ we have $u(x - \Delta x, t) = u(x, t) - \frac{\Delta x \partial u}{\partial x} + \frac{(\Delta x)^2 \partial^2 u}{\partial x^2} + \mathcal{O}((\Delta x)^3)$. We drop the error terms and isolate $\frac{\partial u}{\partial x}$ and obtain $\frac{\partial u}{\partial x} = \frac{u(x, t) - u(x - \Delta x, t)}{\Delta x} \approx \frac{u_i^n - u_{i-1}^n}{\Delta x}$.

We need a centered difference for $\frac{\partial^2 u}{\partial x^2}$. We first get the forward difference which is $u(x + \Delta x, t) = u(x, t) + \frac{\Delta x \partial u}{\partial t} + \frac{(\Delta x)^2 \partial^2 u}{2! \partial x^2} + \mathcal{O}((\Delta x)^3)$. Similarly, we get the backward difference which is $u(x - \Delta x, t) = u(x, t) - \frac{\Delta x \partial u}{\partial t} + \frac{(\Delta x)^2 \partial^2 u}{2! \partial x^2} - \mathcal{O}((\Delta x)^3)$. After adding both the forward and backward difference formula we obtain $u(x + \Delta x, t) + u(x - \Delta x, t) = 2u(x, t) + \frac{\Delta x^2 \partial^2 u}{\partial x^2}$. Now isolating $\frac{\partial^2 u}{\partial x^2}$ we obtain $\frac{\partial^2 u}{\partial x^2} = \frac{u(x + \Delta x, t) + u(x - \Delta x, t) - 2u(x, t)}{\Delta x^2} \approx \frac{u_{i+1}^t + u_{i-1}^t - 2u_i^t}{\Delta x^2}$. Now, combining everything we have the following:

$$\begin{aligned} \frac{u_i^{n+1} - u_i^n}{\Delta t} + a \left(\frac{u_i^n - u_{i-1}^n}{\Delta x} \right) &= \mu \left(\frac{u_{i+1}^t + u_{i-1}^t - 2u_i^t}{\Delta x^2} \right) \\ u_i^{n+1} &= u_i^n - a \Delta t \left(\frac{u_i^n - u_{i-1}^n}{\Delta x} \right) + \mu \Delta t \left(\frac{u_{i+1}^t + u_{i-1}^t - 2u_i^t}{\Delta x^2} \right) \end{aligned}$$

Now let $\nu = \frac{a \Delta t}{\Delta x}$ and $\sigma = \frac{\mu \Delta t}{\Delta x^2}$. Then we have the following explicit finite difference scheme that uses a forward difference in time, centered difference on the diffusion term and first order upwind difference on the advection term.

$$u_i^{n+1} = u_i^n - \nu(u_i^n - u_{i-1}^n) + \sigma(u_{i+1}^t + u_{i-1}^t - 2u_i^t)$$

3b) Assume the solution to the error $u_i^n = G^n e^{i\theta j}$ where $\theta = k\Delta x$. Then, $u_{i+1}^n = G^n e^{i\theta(j+1)} = G^n e^{i\theta j} e^{i\theta}$ and $u_{i-1}^n = G^n e^{i\theta(j-1)} = G^n - e^{i\theta j} e^{i\theta}$. Substituting these values into our scheme from part(a) we obtain $G^{n+1} e^{i\theta j} = G^n e^{i\theta j} (1 - \nu(1 - e^{i\theta}) + \sigma(e^{i\theta} - 2 + e^{-i\theta}))$. Now, subtracting $G^n e^{i\theta j}$ from both sides we obtain $G = 1 - \nu(1 - e^{i\theta}) + \sigma(e^{i\theta} - 2 + e^{-i\theta})$. Now, recall $e^{i\theta} + e^{-i\theta} = 2\cos\theta$ and $e^{i\theta} - e^{-i\theta} = 2i\sin\theta \implies 1 - e^{i\theta} = 1 - (\cos\theta - i\sin\theta) = 1 - \cos\theta + i\sin\theta \implies e^{i\theta} - 2 + e^{-i\theta} = 2\cos\theta - 2$. Substituting these values into our equation for G we have $G = 1 - \nu(1 - \cos\theta + i\sin\theta) + \sigma(2\cos\theta - 2)$. Note, the real part of G here is $1 - \nu(1 - \cos\theta) + \sigma(2\cos\theta - 2)$ and the imaginary part is $\nu i\sin\theta$.

From the lecture notes we know for stability we require $|G| \leq 1$. Then, $|G|^2 = |(1 - \nu(1 - \cos\theta) + \sigma(2\cos\theta - 2))^2 + (\nu i\sin\theta)^2|$. This is an equation on $\theta \in [0, \pi]$ so suppose $\theta = \pi$. Then $|G|^2 = |(1 - \nu(2) + \sigma(-4))^2| = |1 - 2\nu - 4\sigma| \leq 1 \implies 2\nu + 4\sigma \leq 2 \implies \nu + 2\sigma \leq 1$. Hence, the numerical scheme proposed in part(a) is stable as long as $\nu + 2\sigma \leq 1$.

3c) We present our findings from the convergence study in the following tables.

Δx	Δt	N_T	ν	σ	L_2 Error
0.100000	0.08888889	45	0.8889	0.0178	6.426×10^{-2}
0.066667	0.05970149	67	0.8955	0.0269	4.316×10^{-2}
0.050000	0.04494382	89	0.8989	0.0360	3.258×10^{-2}

Table 1: Results for $\mu = 0.002$

Δx	ν	σ	$\nu + 2\sigma$	L_2 Error
0.100000	0.4494	0.0090	0.4674	2.262×10^{-1}
0.066667	0.6742	0.0202	0.7146	1.147×10^{-1}
0.050000	0.8989	0.0360	0.9708	3.258×10^{-2}

Table 2: Accuracy estimates for $\mu = 0.002$ on a log-log slope of ≈ 2.722

Δx	Δt	N_T	ν	σ	L_2 Error
0.100000	0.08888889	45	0.8889	0.0444	5.684×10^{-2}
0.066667	0.05970149	67	0.8955	0.0672	1.435×10^{-1}
0.050000	0.04494382	89	0.8989	0.0899	6.828×10^2

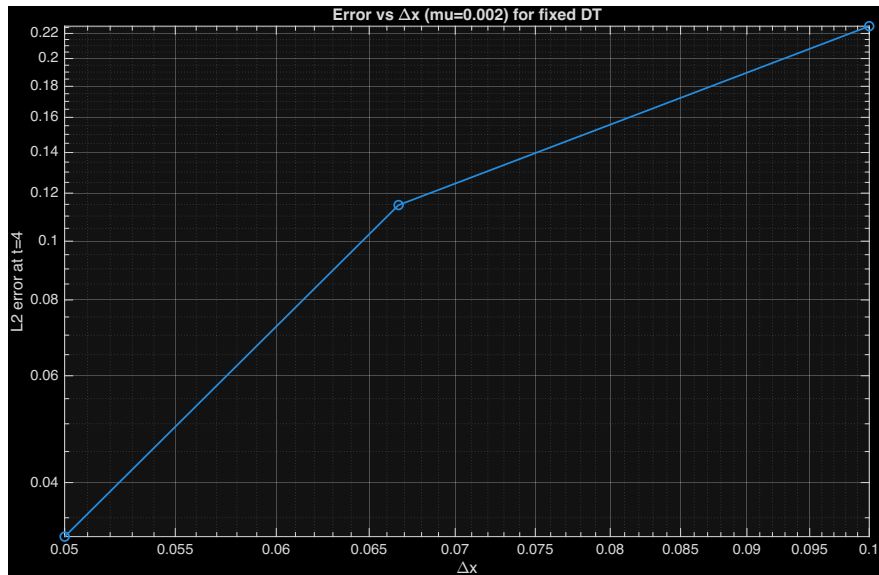
Table 3: Results for $\mu = 0.005$

Δx	ν	σ	$\nu + 2\sigma$	L_2 Error
0.100000	0.4494	0.0225	0.4944	2.056×10^{-1}
0.066667	0.6742	0.0506	0.7753	1.020×10^{-1}
0.050000	0.8989	0.0899	1.0787	6.828×10^2

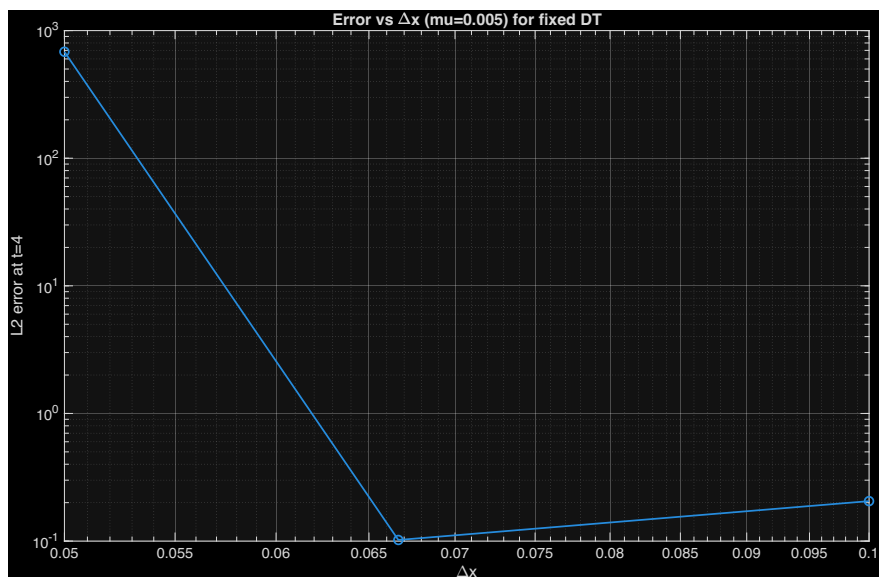
Table 4: Accuracy estimates for $\mu = 0.005$ on a log-log slope of ≈ -10.816

Δx	ν_{\max}
0.100000	0.9091
0.066667	0.8696
0.050000	0.8333

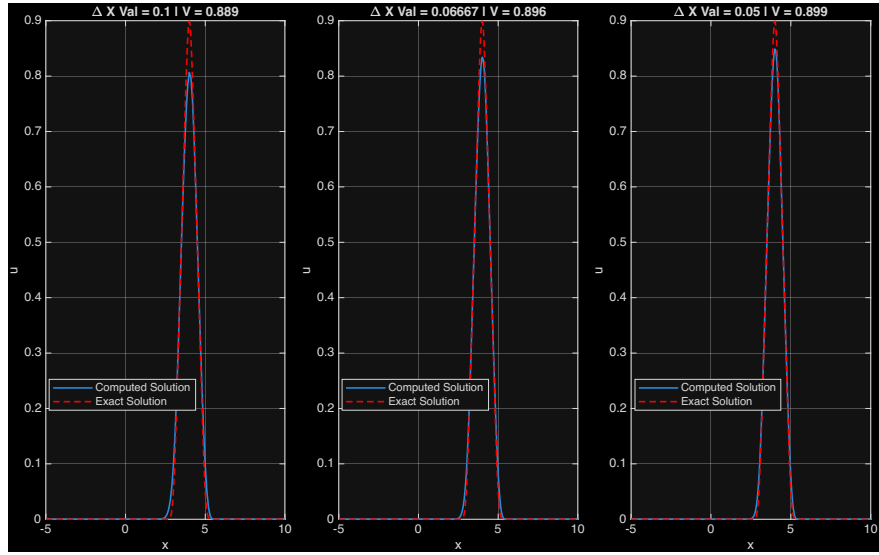
Table 5: Max stable CFL values satisfying $\nu + 2\sigma \leq 1$



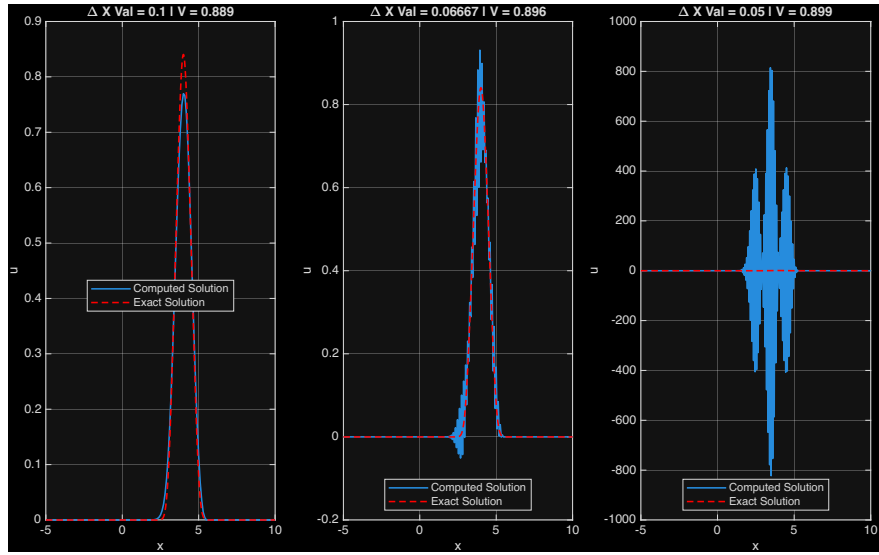
(a) Error vs Fixed DT for $\mu = 0.002$



(b) Error vs Fixed DT for $\mu = 0.005$



(a) Computed Solution vs Exact solution for fixed ν and varying Δx values for $\mu = 0.002$



(b) Computed Solution vs Exact solution for fixed ν and varying Δx values for $\mu = 0.005$

Code for convergence study.